Electronic Supplementary Material (ESI) for ChemComm.

Supporting Information

Subvalent mixed Si_xGe_y oligomers: $(Cl_3Si)_4Ge$ and $Cl_2(Me_2EtN)SiGe(SiCl_3)_2$

Chantal Kunkel, Michael Bolte, Hans-Wolfram Lerner, Philipp Albert, and Matthias Wagner*

Table of contents:

1 General Considerations

All reactions were carried out under an inert-gas atmosphere (dry argon or nitrogen) using standard Schlenk or glovebox techniques. Commercially available substances were used as received. $(Cl_3Si)_4Si$,[S1] $[nBu_4N][(Cl_3Si)_3C]$,[S2] $[nBu_4N][(Cl_3Si)_3Ge]$,[S3] and $AlCl_3$[S4] were synthesized according to literature. Thermolabile compounds were stored in a freezer (–78 °C, –30 °C), in dry-ice baths (–78 °C), or in an *i*PrOH bath connected to a cryostat system (Julabo Haake F6). Solvents were dried over Na metal (*n*-hexane) or CaH_2 (CH_2Cl_2) and either freshly distilled prior to use or stored over molecular sieves (4 Å). C_6D_6 and CD_2Cl_2 were stored over molecular sieves (4 Å). NMR spectra were recorded on a Bruker Avance III HD 500 MHz spectrometer, equipped with a Prodigy BBO 500 S1 probe. $^{1}H/^{13}C\{^{1}H\}$ NMR spectra were referenced against (residual) solvent signals (C_6D_6: 7.16 ppm/128.06 ppm; CD_2Cl_2: 5.32/53.84 ppm).[S5] ^{27}Al NMR spectra were calibrated against external $Al(NO_3)_3$ in D_2O ($\delta(^{27}Al) = 0$).[S6] ^{29}Si NMR spectra were calibrated against external $Si(CH_3)_4$ ($\delta(^{29}Si) = 0$); whenever present, $SiCl_4$ ($\delta(^{29}Si) = -18.9$)[S7] was used as internal standard. Abbreviations: s = singlet, t = triplet, q = quartet, m = multiplet, br = broad signal, n.o. = not observable.

2 Synthetic procedures

2.1 Synthesis of $(Cl_3Si)_4Ge$, 1

An ampoule, equipped with a magnetic stirring bar, was charged with $[n\mathrm{Bu}_4\mathrm{N}][(\mathrm{Cl}_3\mathrm{Si})_3\mathrm{Ge}]$ (0.600 g, 0.835 mmol, 1.0 eq), $AlCl_3$ (0.114 g, 0.855 mmol, 1.0 eq), $SiCl_4$ (7.15 g, 42.1 mmol, 50.4 eq), and CH_2Cl_2 (5.0 mL). The ampoule was flame-sealed under reduced pressure and the orange solution was stirred for 24 h. Afterwards, the ampoule was opened, its content transferred to a Schlenk vessel, and all volatiles were removed under reduced pressure. Extraction of the solid, orange-colored residue with boiling *n*-hexane (3x40 mL) in the glovebox afforded **1** as a colorless solid. Yield: 0.463 g (0.759 mmol, 91%).

The non-extractable solid was dissolved in CD_2Cl_2 and found to consist essentially of $[n\mathrm{Bu}_4\mathrm{N}][\mathrm{AlCl}_4]$ (^{1}H, ^{13}C{^{1}H}, and ^{27}Al{^{1}H} NMR spectroscopy; quantitative yield relative to $AlCl_3$).

Note: 1) The reaction was also performed with 6 or 22 eq of $SiCl_4$. We observed an increase in the yield of **1** with increasing amount of $SiCl_4$ present. 2) It is strongly recommended to use freshly prepared (rather than commercial) $AlCl_3$, and a sealed glass ampoule (rather than a Schlenk tube connected to an overpressure valve) as reaction vessel. CAUTION: Appropriate safety precautions should be observed to avoid overpressure inside the ampoule.

^{29}Si NMR (99.4 MHz, CD_2Cl_2, 298 K): δ = 3.9 (s; $(Cl_3\mathit{Si})_4Ge$)

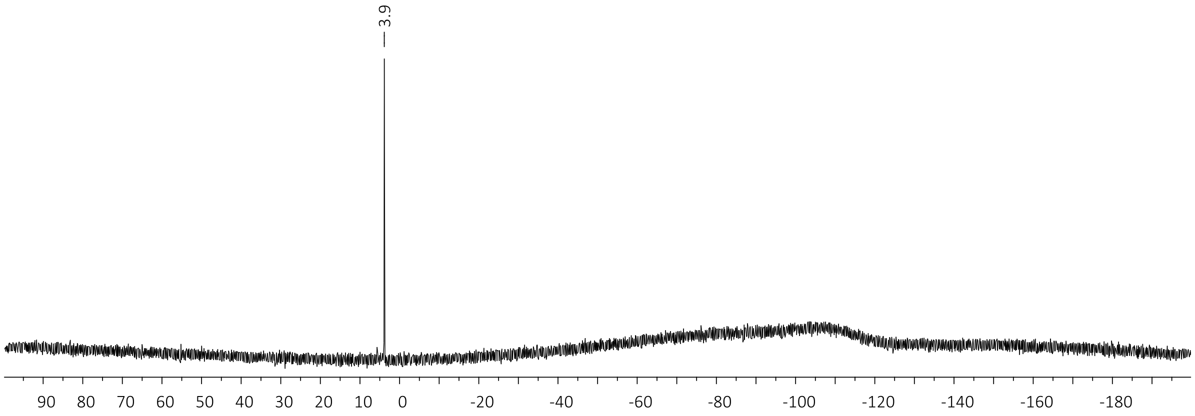

Figure S1: ^{29}Si{^{1}H} NMR spectrum of **1** (99.4 MHz, CD_2Cl_2, 298 K)

NMR spectroscopic investigations of mixtures of [nBu$_4$N][(Cl$_3$Si)$_3$Ge] and AlCl$_3$ in CD$_2$Cl$_2$

freshly prepared mixture

^{1}H NMR (500.18 MHz, CD$_2$Cl$_2$, 298 K): δ = 3.12-3.08 (m, 2H; NCH_2CH$_2$), 1.65-1.59 (m, 2H; NCH$_2$CH_2), 1.48–1.42 (m, 2H; CH_2CH$_3$), 1.02 (t, 3H, $^3J_{HH}$ = 7.4 Hz; CH$_2$CH_3)

^{27}Al{^{1}H} NMR (130.3 MHz, CD$_2$Cl$_2$, 298 K): δ = 115.1 (s; [(Cl$_3$Si)$_3$GeAlCl$_3$]$^-$), 103.8 (s; [AlCl$_4$]$^-$)

^{29}Si{^{1}H} NMR (99.4 MHz, CD$_2$Cl$_2$, 298 K): δ = 14.0 (br; [(Cl$_3$$Si$)$_3$GeAlCl$_3$]$^-$)

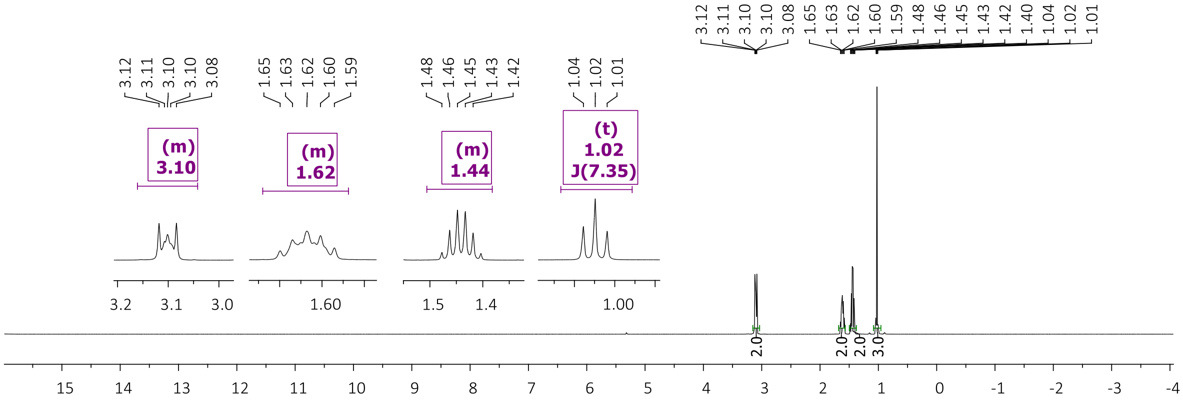

Figure S2: ^{1}H NMR spectrum (500.18 MHz, CD$_2$Cl$_2$, 298 K) of a freshly prepared mixture of [nBu$_4$N][(Cl$_3$Si)$_3$Ge] and AlCl$_3$.

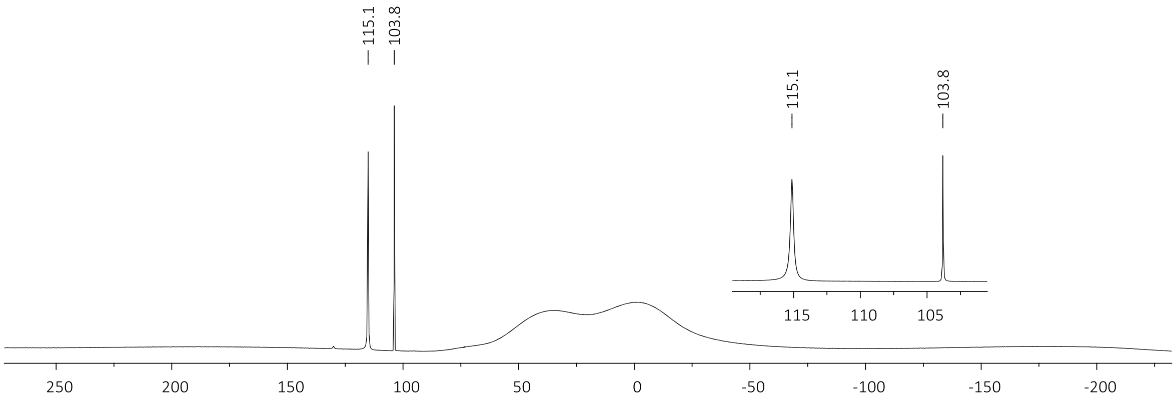

Figure S3: ^{27}Al{^{1}H} NMR spectrum (130.3 MHz, CD$_2$Cl$_2$, 298 K) of a freshly prepared mixture of [nBu$_4$N][(Cl$_3$Si)$_3$Ge] and AlCl$_3$.

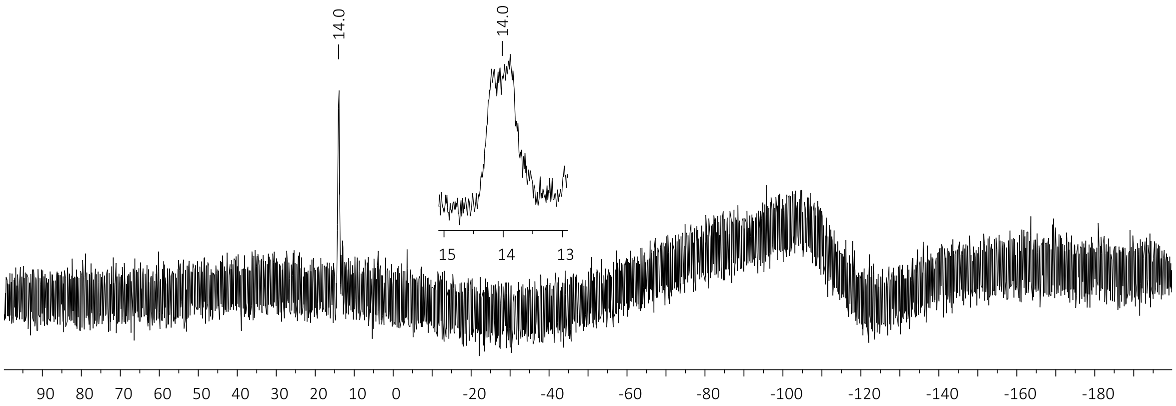

Figure S4: ^{29}Si{^{1}H} NMR spectrum (99.4 MHz, CD_2Cl_2, 298 K) of a freshly prepared mixture of [*n*Bu_4N][$(Cl_3Si)_3Ge$] and $AlCl_3$.

*after partial conversion to **1**, [$AlCl_4$]$^–$, and $SiCl_4$*

^{1}H NMR (500.18 MHz, CD_2Cl_2, 298 K): *δ* = 3.12-3.09 (m, 2H; NC*H*$_2$CH$_2$), 1.65-1.58 (m, 2H; NCH$_2$C*H*$_2$), 1.47-1.41 (m, 2H; C*H*$_2$CH$_3$), 1.02 (t, 3H, $^{3}J_{HH}$ = 7.4 Hz; CH$_2$C*H*$_3$)

^{27}Al{^{1}H} NMR (130.3 MHz, CD_2Cl_2, 298 K): *δ* = 115.1 (s; [$(Cl_3Si)_3Ge$*Al*Cl_3]$^–$), 103.8 (s; [*Al*Cl_4]$^–$)

^{29}Si{^{1}H} NMR (99.4 MHz, CD_2Cl_2, 298 K): *δ* = 14.0 (br; [$(Cl_3$*Si*$)_3GeAlCl_3$]$^–$), 3.8 (s, $(Cl_3$*Si*$)_4Ge$), –18.9 (*Si*Cl_4)

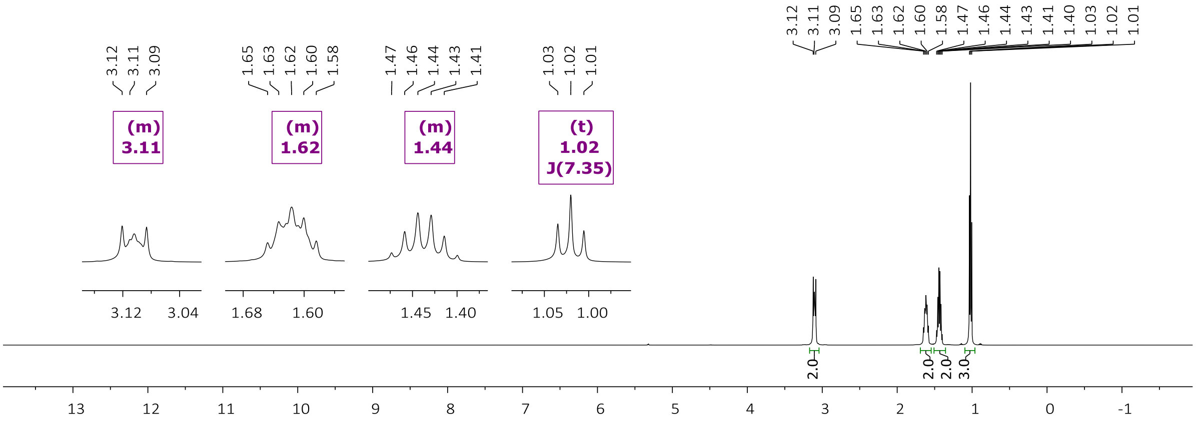

Figure S5: ^{1}H NMR spectrum (500.18 MHz, CD_2Cl_2, 298 K) of a reaction mixture of [*n*Bu_4N][$(Cl_3Si)_3Ge$] and $AlCl_3$ after partial conversion of the initially formed [*n*Bu_4N][$(Cl_3Si)_3GeAlCl_3$] to **1**, [*n*Bu_4N][$AlCl_4$], and $SiCl_4$.

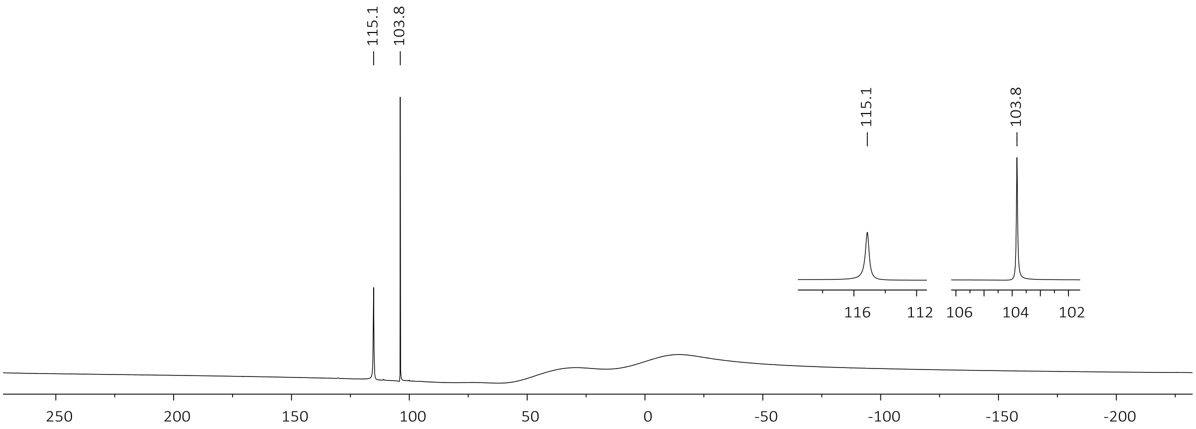

Figure S6: ^{27}Al{^{1}H} NMR spectrum (130.3 MHz, CD_2Cl_2, 298 K) of a reaction mixture of [*n*Bu$_4$N][($Cl_3Si)_3$Ge] and $AlCl_3$ after partial conversion of the initially formed [*n*Bu$_4$N][($Cl_3Si)_3$GeAlCl$_3$] to **1**, [*n*Bu$_4$N][AlCl$_4$], and $SiCl_4$.

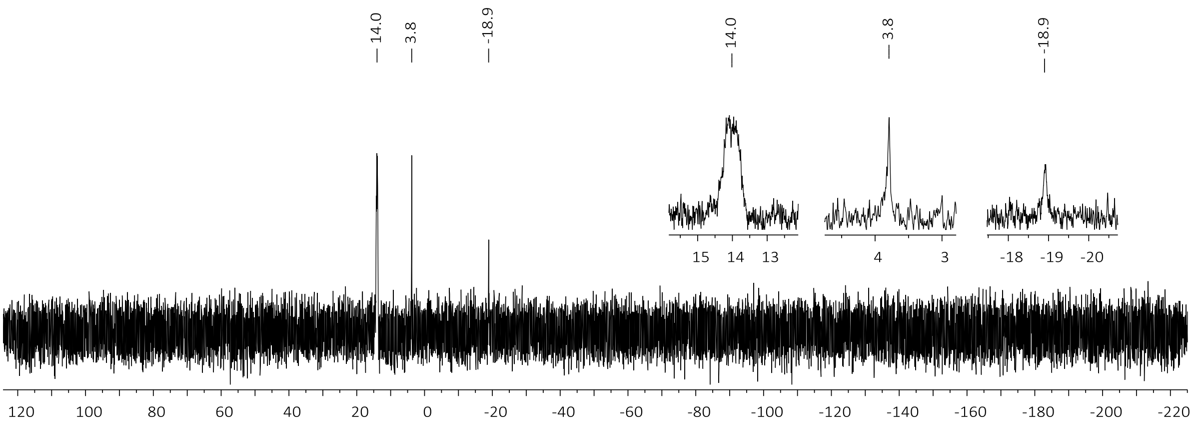

Figure S7: ^{29}Si{^{1}H} NMR spectrum (99.4 MHz, CD_2Cl_2, 298 K) of a reaction mixture of [*n*Bu$_4$N][($Cl_3Si)_3$Ge] and $AlCl_3$ after partial conversion of the initially formed [*n*Bu$_4$N][($Cl_3Si)_3$GeAlCl$_3$] to **1**, [*n*Bu$_4$N][AlCl$_4$], and $SiCl_4$.

after complete conversion to ***1****, [AlCl$_4$]$^-$, and SiCl$_4$*

^{1}H NMR (500.18 MHz, CD_2Cl_2, 298 K): *δ* = 3.14-3.11 (m, 2H; NC*H*$_2$CH$_2$), 1.66-1.59 (m, 2H; NCH$_2$C*H*$_2$), 1.47–1.40 (m, 2H; C*H*$_2$CH$_3$), 1.02 (t, 3H, $^3J_{HH}$ = 7.4 Hz; CH$_2$C*H*$_3$)

^{27}Al{^{1}H} NMR (130.3 MHz, CD_2Cl_2, 298 K): *δ* = 103.8 (s; [*Al*Cl$_4$]$^-$)

^{29}Si{^{1}H} NMR (99.4 MHz, CD_2Cl_2, 298 K): *δ* = 3.8 (s, (Cl$_3$*Si*)$_4$Ge), –18.9 (*Si*Cl$_4$)

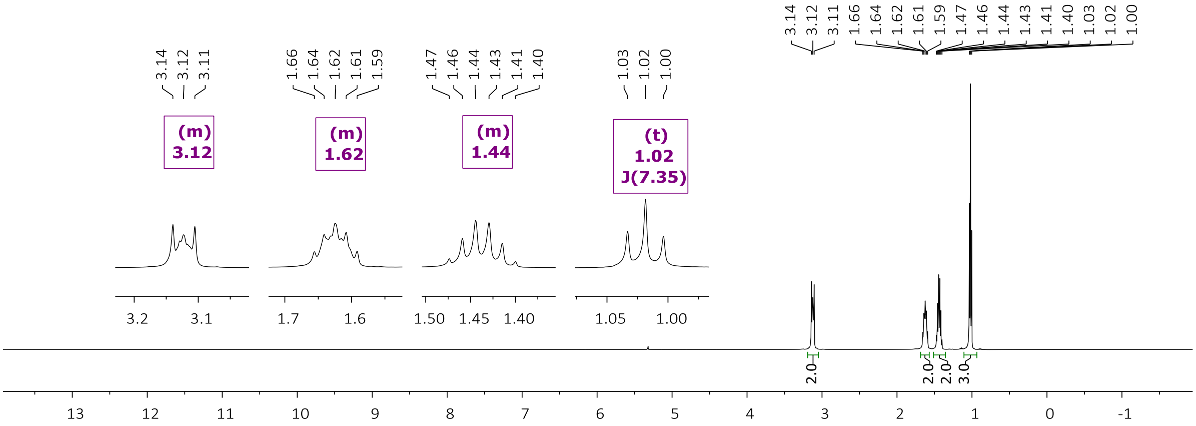

Figure S8: ^{1}H NMR spectrum (500.18 MHz, CD_2Cl_2, 298 K) of a reaction mixture of [*n*Bu_4N][$(Cl_3Si)_3Ge$] and $AlCl_3$ after complete conversion of the initially formed [*n*Bu_4N][$(Cl_3Si)_3GeAlCl_3$] to **1**, [*n*Bu_4N][$AlCl_4$], and $SiCl_4$.

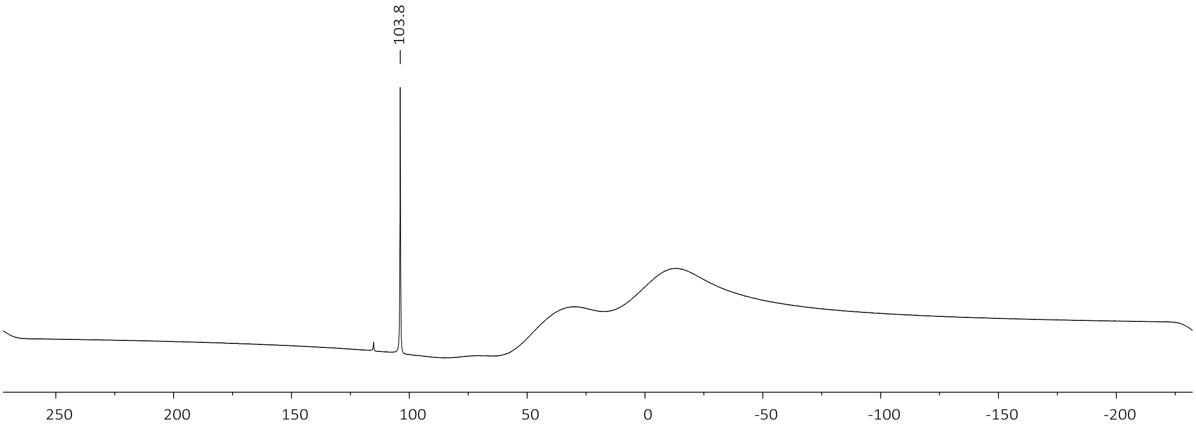

Figure S9: ^{27}Al{^{1}H} NMR spectrum (130.3 MHz, CD_2Cl_2, 298 K) of a reaction mixture of [*n*Bu_4N][$(Cl_3Si)_3Ge$] and $AlCl_3$ after complete conversion of the initially formed [*n*Bu_4N][$(Cl_3Si)_3GeAlCl_3$] to **1**, [*n*Bu_4N][$AlCl_4$], and $SiCl_4$.

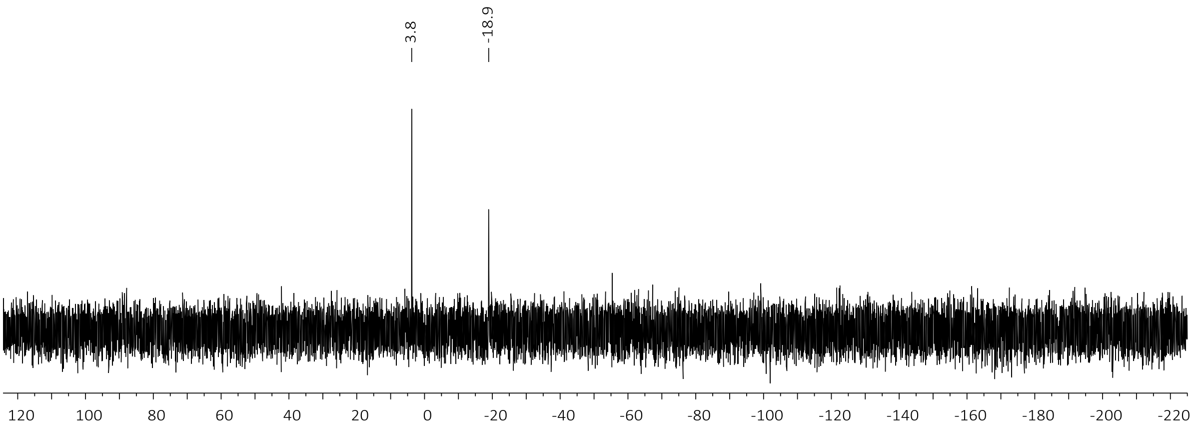

Figure S10: ^{29}Si{^{1}H} NMR spectrum (99.4 MHz, CD_2Cl_2, 298 K) of a reaction mixture of [*n*Bu_4N][$(Cl_3Si)_3Ge$] and $AlCl_3$ after complete conversion of the initially formed [*n*Bu_4N][$(Cl_3Si)_3GeAlCl_3$] to **1**, [*n*Bu_4N][$AlCl_4$], and $SiCl_4$.

2.2 Synthesis of the adduct between [*n*Bu$_4$N][(Cl$_3$Si)$_3$C] and AlCl$_3$

An NMR tube was charged with [*n*Bu$_4$N][(Cl$_3$Si)$_3$C] (0.050 g, 0.076 mmol, 1.0 eq), AlCl$_3$ (0.020 g, 0.150 mmol, 2.0 eq), and CD$_2$Cl$_2$ (0.6 mL). The NMR tube was flame-sealed and NMR spectra were recorded. The ^{29}Si NMR spectrum showed a complete conversion of [(Cl$_3$Si)$_3$C]$^-$ to [(Cl$_3$Si)$_3$CAlCl$_3$]$^-$. In addition to [(Cl$_3$Si)$_3$CAlCl$_3$]$^-$, the [AlCl$_4$]$^-$ anion could also be detected in the ^{27}Al NMR spectrum.

Note: 2 eq of AlCl$_3$ are necessary to achieve a complete conversion of [(Cl$_3$Si)$_3$C]$^-$ to [(Cl$_3$Si)$_3$CAlCl$_3$]$^-$. In all reactions of [(Cl$_3$Si)$_3$C]$^-$ with AlCl$_3$, [AlCl$_4$]$^-$ was observable in the ^{27}Al NMR spectra. Single crystals of [(Cl$_3$Si)$_3$CAlCl$_3$]$^-$ were obtained from a reaction of [(Cl$_3$Si)$_3$C]$^-$ with AlCl$_3$ (1 eq).

^{1}H NMR (500.18 MHz, CD$_2$Cl$_2$, 298 K): δ = 3.11-3.08 (m, 2H; NC*H*$_2$), 1.64-1.58 (m, 2H; NCH$_2$C*H*$_2$), 1.46-1.41 (m, 2H; C*H*$_2$CH$_3$), 1.02 (t, 3H, $^3J_{\mathrm{HH}}$ = 7.3 Hz; CH$_2$C*H*$_3$)

^{13}C{^{1}H} NMR (125.8 MHz, CD$_2$Cl$_2$, 298 K): δ = 59.4 (s; N*C*H$_2$), 24.2 (s; NCH$_2$*C*H$_2$), 20.0 (s; *C*H$_2$CH$_3$), 13.7 (s; CH$_2$*C*H$_3$), n.o. (Si$_3$*C*Al)

^{27}Al NMR (130.3 MHz, CD$_2$Cl$_2$, 298 K): δ = 113.2 (br; [(Cl$_3$Si)$_3$C*Al*Cl$_3$]$^-$), 106.8 (s; [*Al*Cl$_4$]$^-$)

^{29}Si NMR (99.4 MHz, CD$_2$Cl$_2$, 298 K): δ = –3.5 (s; *Si*Cl$_3$)

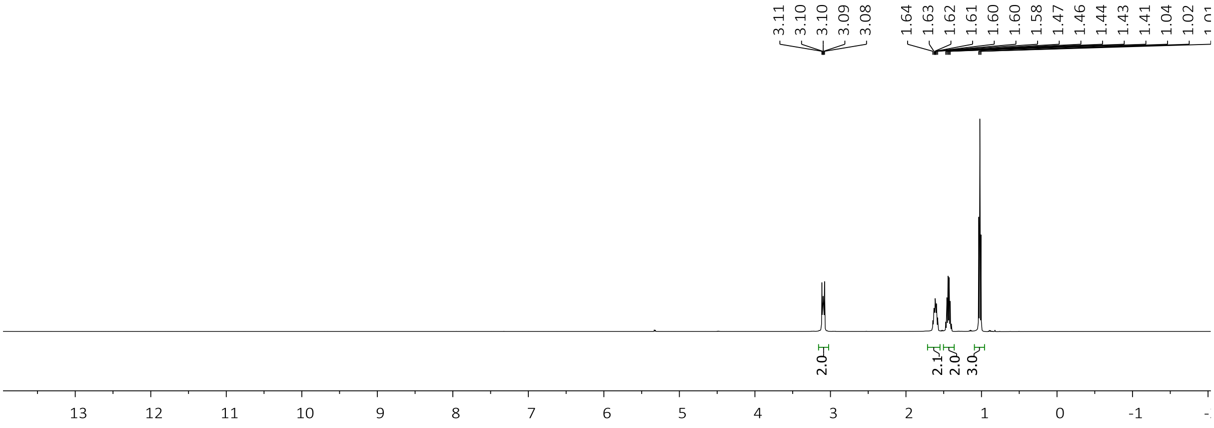

Figure S11: ^{1}H NMR spectrum (500.18 MHz, CD$_2$Cl$_2$, 298 K) of the reaction mixture of [*n*Bu$_4$N][(Cl$_3$Si)$_3$C] and AlCl$_3$.

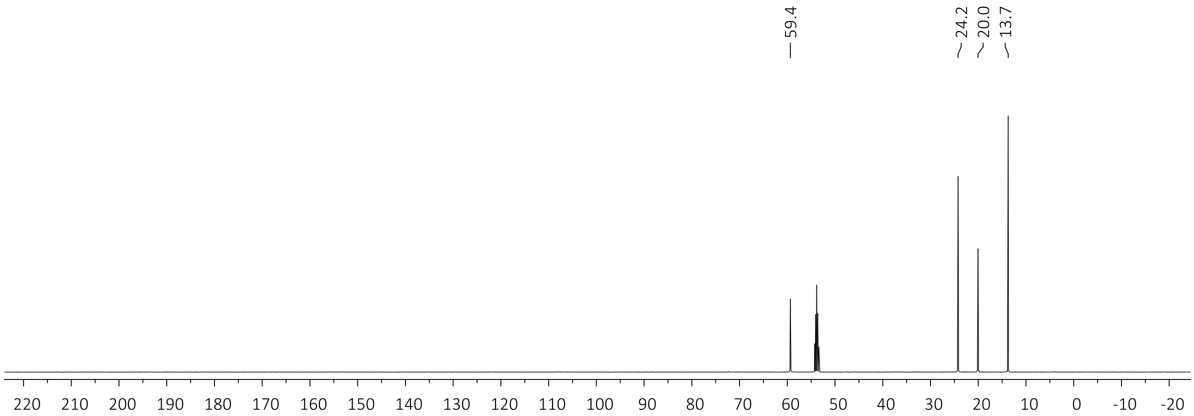

Figure S12: $^{13}C\{^1H\}$ NMR spectrum (125.8 MHz, CD_2Cl_2, 298 K) of the reaction mixture of $[nBu_4N][(Cl_3Si)_3C]$ and $AlCl_3$.

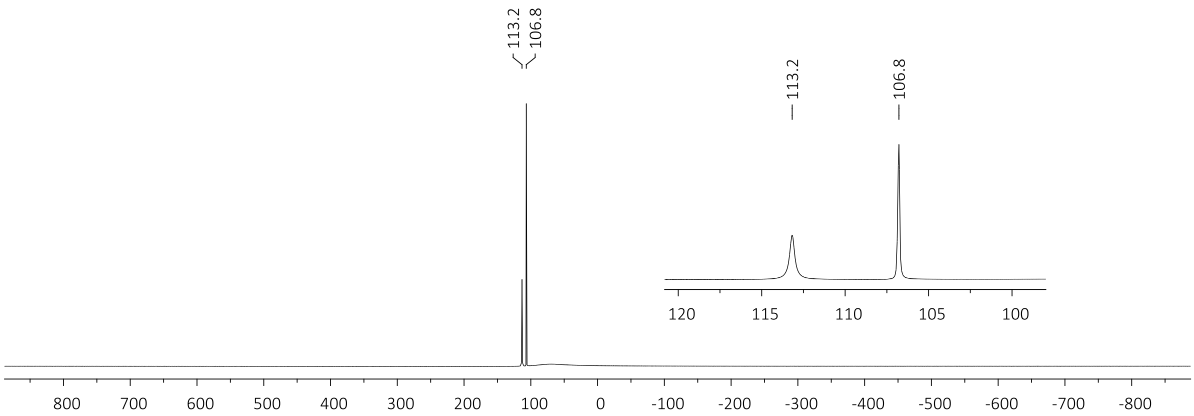

Figure S13: ^{27}Al NMR spectrum (130.3 MHz, CD_2Cl_2, 298 K) of the reaction mixture of $[nBu_4N][(Cl_3Si)_3C]$ and $AlCl_3$.

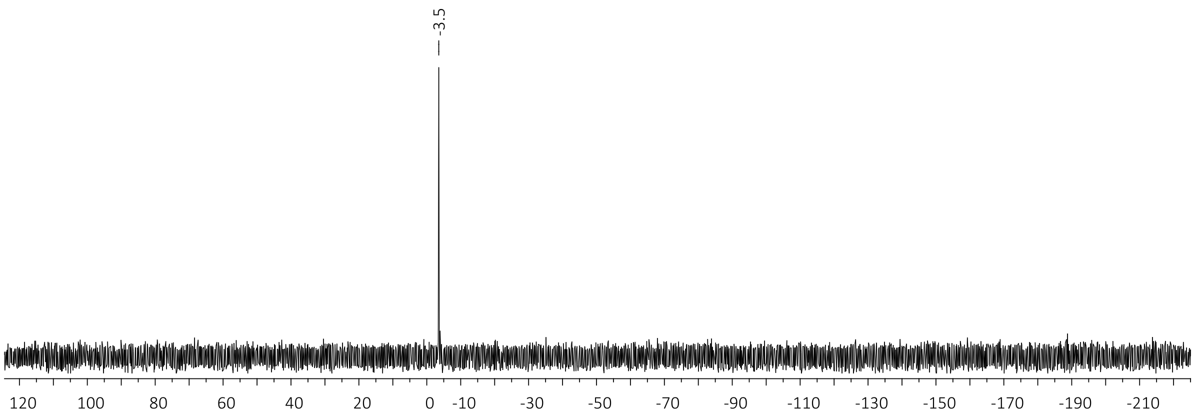

Figure S14: ^{29}Si NMR spectrum (99.4 MHz, CD_2Cl_2, 298 K) of the reaction mixture of $[nBu_4N][(Cl_3Si)_3C]$ and $AlCl_3$.

2.3 Synthesis of $Cl_2(Me_2EtN)SiGe(SiCl_3)_2$, 2

Method 1: from ***1*** *and* Me_2EtN**.** An NMR tube was charged with neat **1** (0.080 g, 0.131 mmol, 1.0 eq) and immersed in a Dewar flask containing liquid N_2 (–196 °C). A solution of Me_2EtN (0.018 g, 0.246 mmol, 1.9 eq) in C_6D_6 (0.6 mL) was added. The NMR tube was flame-sealed, allowed to warm until the C_6D_6 liquefied, and placed into the NMR spectrometer precooled to 10 °C. NMR spectra were recorded at 10 °C, revealing that **2** and $SiCl_4$ had formed.

Note regarding Method 1: According to NMR, the conversion **1** → **2** was essentially quantitative.

^{1}H NMR (500.18 MHz, C_6D_6, 283 K): δ = 2.42 (q, 2H, $^3J_{HH}$ = 7.2 Hz; CH_2CH_3), 1.65 (s, 6H; $N(CH_3)_2$), 0.10 (t, 3H, $^3J_{HH}$ = 7.2 Hz; CH_2CH_3)

^{13}C{^{1}H} NMR (125.8 MHz, C_6D_6, 283 K): δ = 52.6 (s; CH_2CH_3), 41.7 (s; $N(CH_3)_2$), 6.0 (s; CH_2CH_3)

^{29}Si{^{1}H} NMR (99.4 MHz, C_6D_6, 283 K): δ = 45.3 (s; $SiCl_2$), 27.7 (s; $SiCl_3$), –18.9 ($SiCl_4$)

^{1}H/^{29}Si HMBC NMR (500.2/99.4 MHz, C_6D_6, 283 K): cross peaks were observed between the couples δ = 2.42/45.3 and 1.65/45.3.

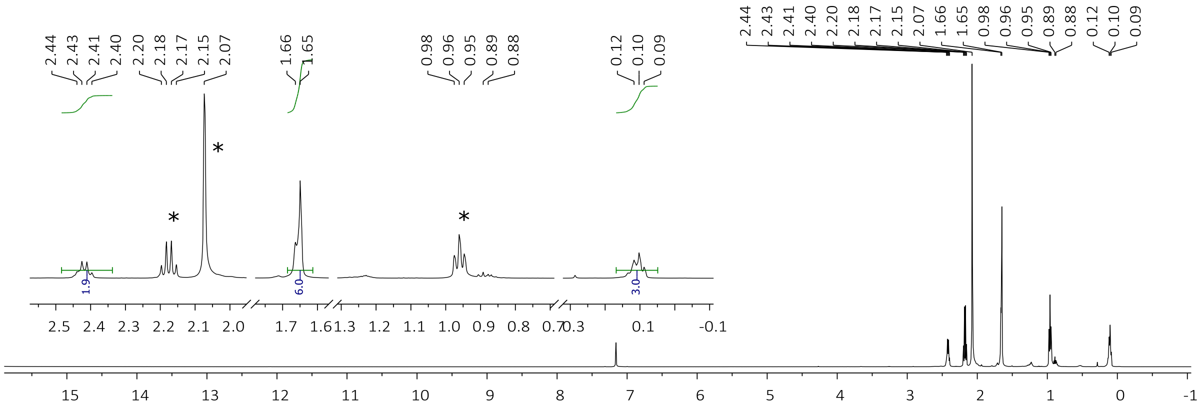

Figure S15: ^{1}H NMR spectrum (500.18 MHz, C_6D_6, **283 K**) of the reaction mixture of **1** and Me_2EtN. *) Me_2EtN

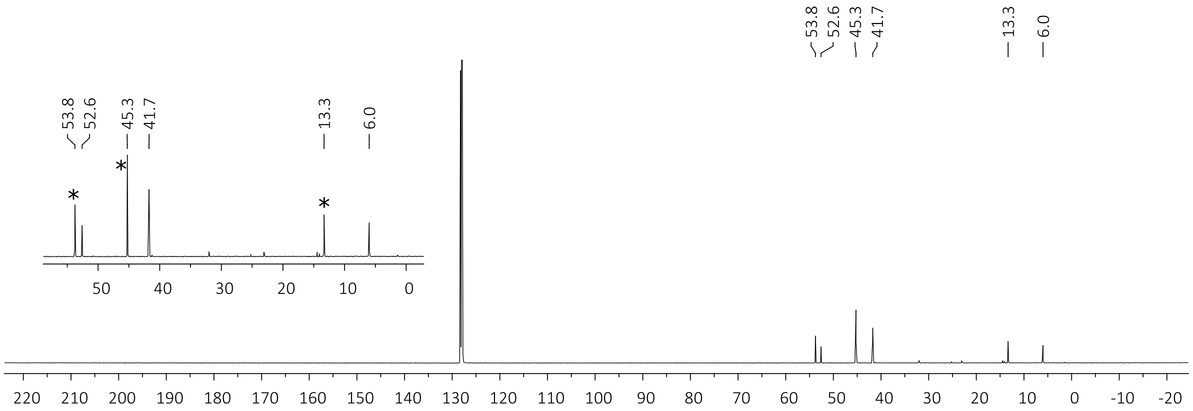

Figure S16: $^{13}C\{^{1}H\}$ NMR spectrum (125.8 MHz, C_6D_6, **283 K**) of the reaction mixture of **1** and Me_2EtN. *) Me_2EtN

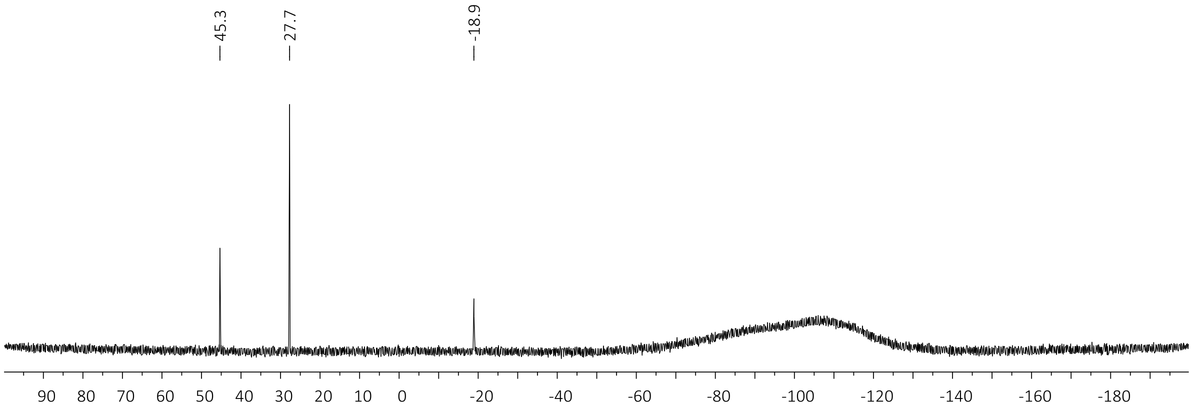

Figure S17: $^{29}Si\{^{1}H\}$ NMR spectrum (99.4 MHz, C_6D_6, **283 K**) of the reaction mixture of **1** and Me_2EtN.

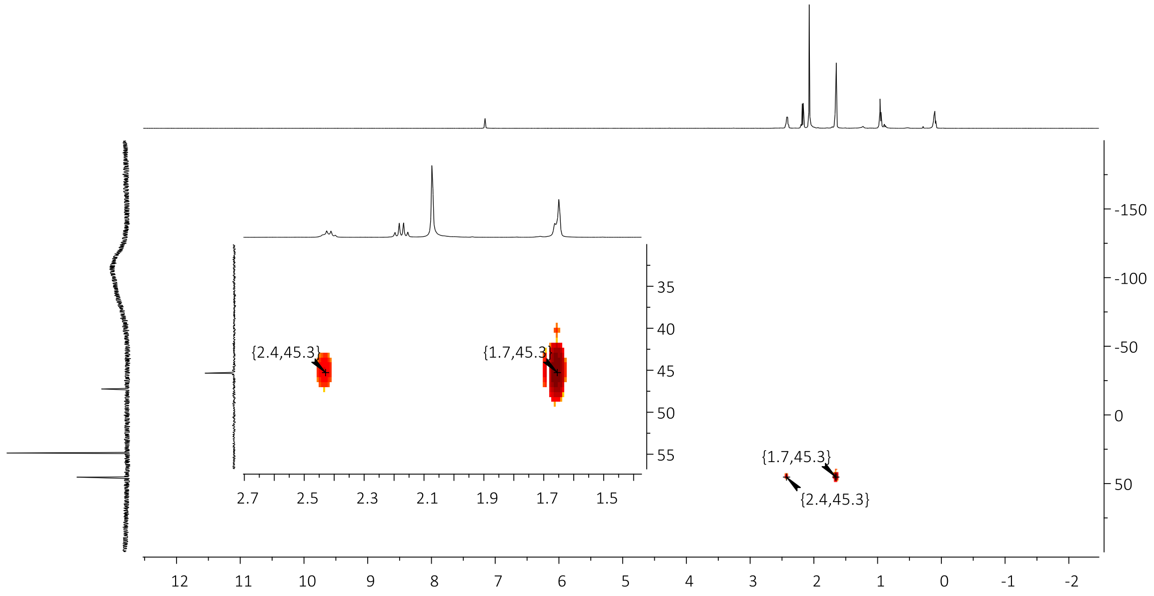

Figure S18: $^{1}H/^{29}Si$ HMBC NMR spectrum (500.2/99.4 MHz, C_6D_6, **283 K**) of the reaction mixture of **1** and Me_2EtN.

Method 2: from Si_2Cl_6, $GeCl_4$, and Me_2EtN. A Schlenk tube was charged with Si_2Cl_6 (2.45 g, 9.12 mmol, 3.8 eq), $GeCl_4$ (0.513 g, 2.39 mmol, 1.0 eq), and CH_2Cl_2 (8.0 mL). Upon addition of Me_2EtN (0.30 mL, 0.203 g, 2.77 mmol, 1.2 eq) at room temperature with vigorous stirring, the colorless solution instantaneously turned pale yellow. Immediately after the addition was complete, the solution was cooled to –78 °C. Stirring was continued at –78 °C for 1 h. Crystals of **2** suitable for X-ray analysis were grown by slowly cooling the sample from –30 °C to –45 °C in a cryostat. The pale yellow mother liquor was removed with a syringe (at –45 °C). All remaining volatiles were removed under reduced pressure and **2** was isolated in the form of colorless crystal blocks (cooling should be maintained all the time). Sample preparation for NMR spectroscopic investigation was performed at –78 °C and the NMR spectra were recorded at –30 °C. When the sample was subsequently warmed to room temperature, a red oil formed. The NMR tube was opened and MeOH was added. All volatiles were evaporated under ambient pressure. The colorless solid residue was analyzed by EDX, confirming the presence of germanium.

Note regarding Method 2: A high dilution of the reaction mixture seems to be crucial for suppressing the formation of poly(chlorosilane)s (red oil). The yield of **2** could not be determined, due to the pronounced thermolability of the compound.

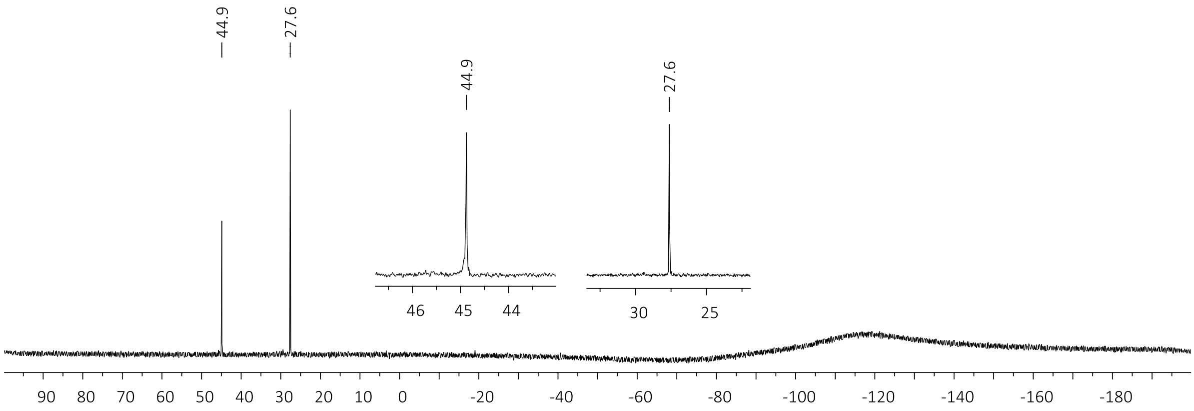

Figure S19: $^{29}Si\{^1H\}$ NMR spectrum (99.4 MHz, CD_2Cl_2, **243 K**) of isolated crystals of **2**. Minor differences in the chemical shift values of the resonances shown in Figures S19 and S17 are either due to the different measurement temperatures or reflect the error margins of the NMR method.

2.4 NMR spectroscopic investigation of a mixture of 1 and $(Cl_3Si)_4Si$

An NMR tube was charged with **1** (0.040 g, 0.066 mmol, 1.0 eq), $(Cl_3Si)_4Si$ (0.038 g, 0.067 mmol, 1.0 eq), and CD_2Cl_2 (0.5 mL). The NMR tube was flame-sealed and NMR spectra were recorded. In the $^{29}Si\{^1H\}$ NMR spectrum, two separate sets of signals can be observed for **1** and $(Cl_3Si)_4Si$.

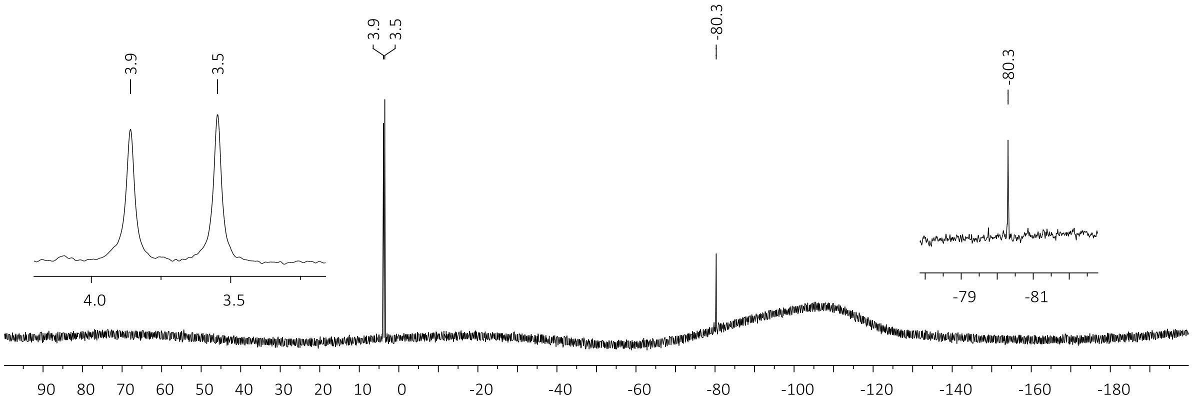

Figure S20: $^{29}Si\{^1H\}$ NMR spectrum (99.4 MHz, CD_2Cl_2, 298 K) of a mixture of **1** and $(Cl_3Si)_4Si$.

2.5 NMR spectroscopic investigation of a mixture of 2 and 2^{Si}

An NMR tube was charged with **1** (0.030 g, 0.049 mmol, 1.0 eq), $(Cl_3Si)_4Si$ (0.028 g, 0.049 mmol, 1.0 eq), and CD_2Cl_2 (0.5 mL). The NMR tube was immersed in a Dewar flask containing liquid N_2 (–196 °C), and a freshly prepared solution of Me_2EtN in CH_2Cl_2 (0.11 mL, 1M, 0.11 mmol, 2.2 eq) was added. The NMR tube was flame-sealed, warmed until the solvent liquefied, and stored at –78 °C. The sample was placed into an NMR spectrometer, precooled to –30 °C. In the $^{29}Si\{^1H\}$ NMR spectrum, two separate sets of signals can be observed for **2** and $\mathbf{2^{Si}}$.[S8] After the measurement at –30 °C, the NMR spectrometer was warmed to –10, 10, and 25 °C to record NMR spectra also at these temperatures.

Note: Solutions of Me_2EtN in CH_2Cl_2/CD_2Cl_2 have to be freshly prepared prior to use. If they are stored over longer periods of time, an activation of the solvent by Me_2EtN is observed (see the NMR and X-ray characterization data of the activation product $[Me_2EtNCH_2Cl]Cl$ in Figures S25, S26, and S30).

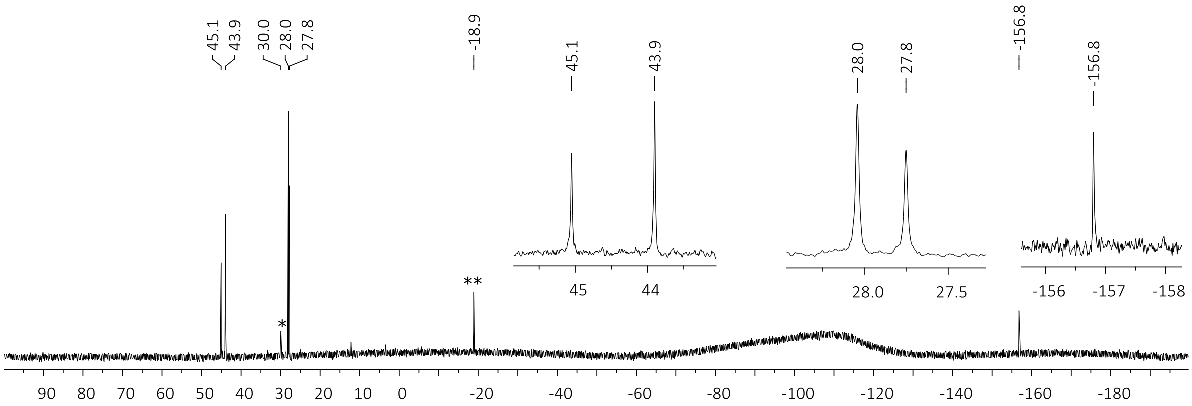

Figure S21: $^{29}Si\{^{1}H\}$ NMR spectrum (99.4 MHz, CD_2Cl_2, **243 K**) of a reaction mixture of $(Cl_3Si)_4Si$ and **1** with Me_2EtN. *) unknown impurity; **) $SiCl_4$.

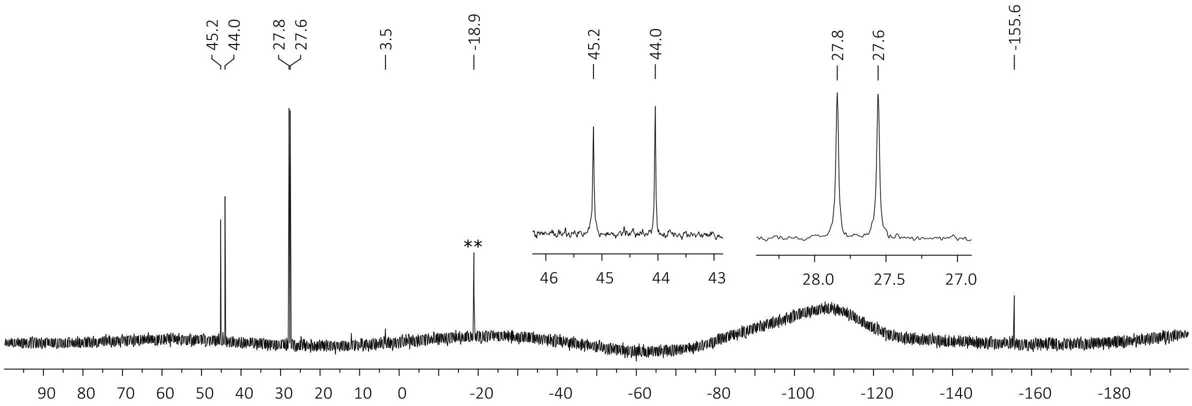

Figure S22: $^{29}Si\{^{1}H\}$ NMR spectrum (99.4 MHz, CD_2Cl_2, **263 K**) of a reaction mixture of $(Cl_3Si)_4Si$ and **1** with Me_2EtN. **) $SiCl_4$.

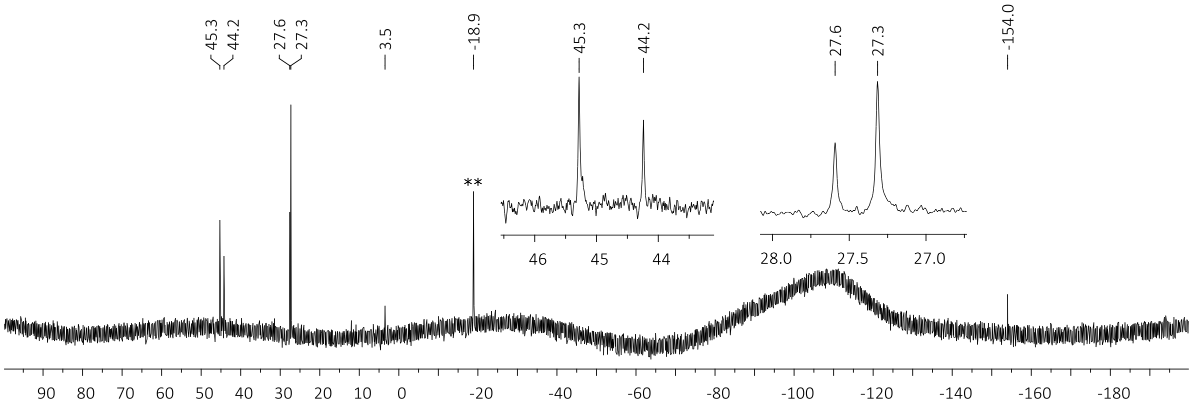

Figure S23: $^{29}Si\{^{1}H\}$ NMR spectrum (99.4 MHz, CD_2Cl_2, **283 K**) of a reaction mixture of $(Cl_3Si)_4Si$ and **1** with Me_2EtN. **) $SiCl_4$.

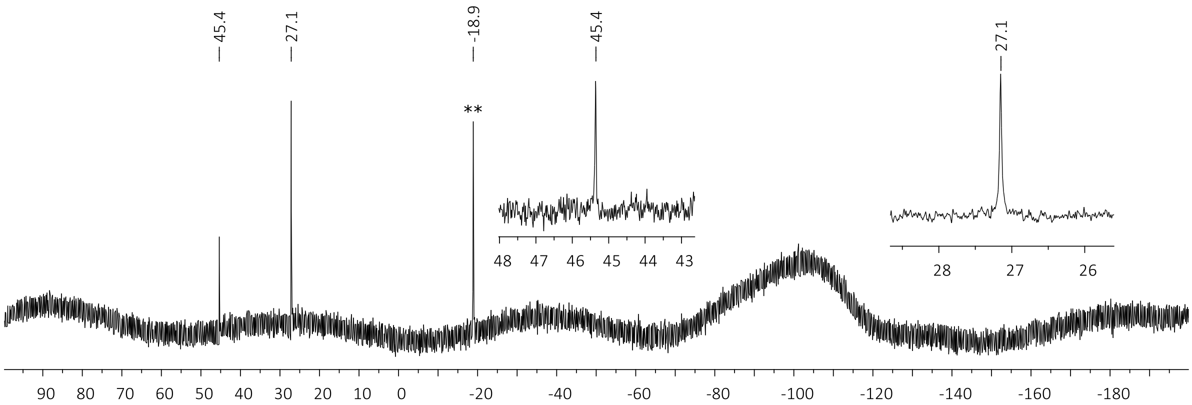

Figure S24: $^{29}Si\{^1H\}$ NMR spectrum (99.4 MHz, CD_2Cl_2, **298 K**) of a reaction mixture of $(Cl_3Si)_4Si$ and **1** with Me_2EtN. **) $SiCl_4$.

2.6 Synthesis of [Me_2EtNCH_2Cl]Cl

A solution of Me_2EtN in CH_2Cl_2 was prepared. Upon storing at room temperature overnight, colorless crystals of [Me_2EtNCH_2Cl]Cl had formed. Sample preparation for X-ray analysis and NMR spectroscopy was carried out under ambient air.

^{1}H NMR (500.18 MHz, CD_2Cl_2, 298 K): δ = 5.95 (s, 2H; CH_2Cl), 3.80 (q, 2H, $^3J_{HH}$ = 7.3 Hz; CH_2CH$_3$), 3.48 (s, 6H; N(CH_3)$_2$), 1.43 (t, 3H, $^3J_{HH}$ = 7.3 Hz; CH$_2$CH_3)

^{13}C{^{1}H} NMR (125.8 MHz, CD_2Cl_2, 298 K): δ = 68.8 (s; CH$_2$Cl), 58.6 (s; CH$_2$CH$_3$), 49.0 (s; N(CH$_3$)$_2$), 8.6 (s; CH$_2$$CH_3$)

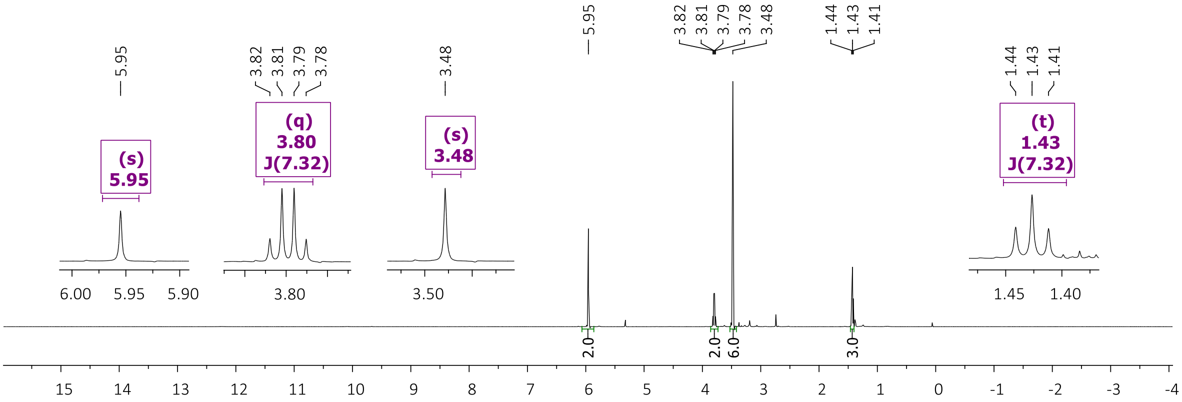

Figure S25: ^{1}H NMR spectrum (500.18 MHz, CD_2Cl_2, 298 K) of [Me_2EtNCH_2Cl]Cl.

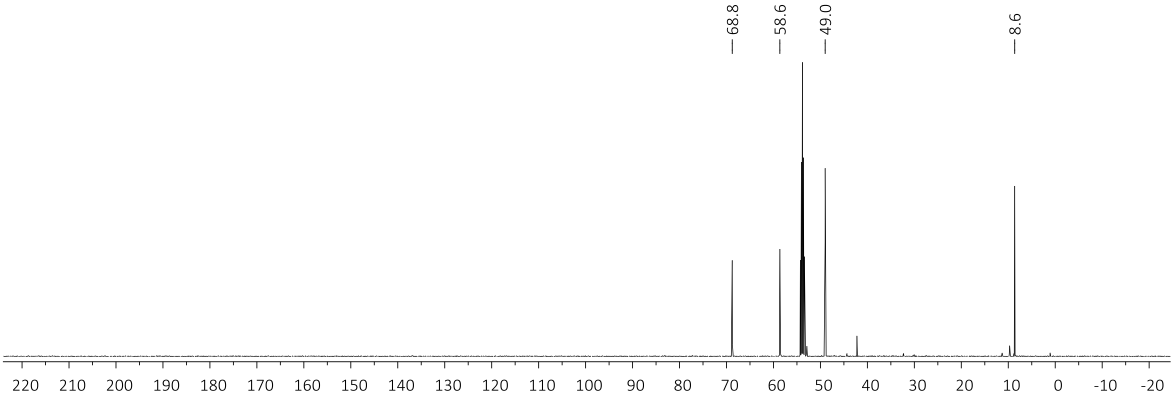

Figure S26: ^{13}C{^{1}H} NMR spectrum (125.8 MHz, CD_2Cl_2, 298 K) of [Me_2EtNCH_2Cl]Cl.

3 X-ray crystal structure analyses

Crystal structure determinations. Data for all structures were collected on a STOE IPDS II two-circle diffractometer with a Genix Microfocus tube with mirror optics using MoK_α radiation (λ = 0.71073 Å). The data were scaled using the frame scaling procedure in the *X-AREA* program system (Stoe & Cie, 2002).[S9] The structures were solved by direct methods using the program *SHELXS* (Sheldrick, 2008) and refined against F^2 *w*ith full-matrix least-squares techniques using the program *SHELXL* (Sheldrick, 2008).[S10]

CCDC files (2105157, 2105158, 2105159) contain the supplementary crystallographic data for this paper and can be obtained free of charge from The Cambridge Crystallographic Data Centre via www.ccdc.cam.ac.uk/data_request/cif.

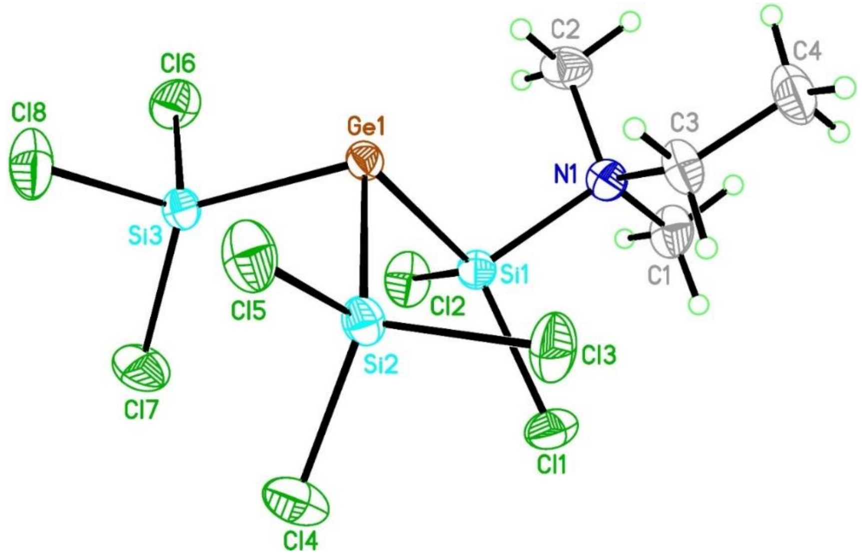

Figure S27: Molecular structure of **2**, in the solid state. Displacement ellipsoids are shown at the 50% probability level. Selected bond lengths [Å] and bond angles [°]: Ge(1)–Si(1) = 2.3929(7), Ge(1)–Si(2) = 2.3692(7), Ge(1)–Si(3) = 2.3792(7), Si(1)–N(1) = 1.908(2); Si(1)–Ge(1)–Si(2) = 95.72(2), Si(1)–Ge(1)–Si(3) = 94.70(2), Si(2)–Ge(1)–Si(3) = 97.85(3), N(1)–Si(1)–Ge(1) = 106.06(7), N(1)–Si(1)–Cl(1) = 100.97(7), N(1)–Si(1)–Cl(2) = 100.97(7), Cl(1)–Si(1)–Cl(2) = 105.51(4), Cl(1)–Si(1)–Ge(1) = 123.52(4), Cl(2)–Si(1)–Ge(1) = 116.36(4); N(1)–Si(1)–Ge(1)–Si(2) = –121.01(7), N(1)–Si(1)–Ge(1)–Si(3) = 140.59(7), Cl(1)–Si(1)–Ge(1)–Si(2) = –5.66(5), Cl(2)–Si(1)–Ge(1)–Si(3) = 29.27(4). **CCDC: 2105157.**

2 crystallizes isomorphous with $\mathbf{2}^{\mathbf{Si}}$.[S8] If the Ge atom is refined as a Si atom, the figures of merit become significantly worse: *R*1 = 0.2677, *wR*2 = 0.5746 (instead of *R1* = 0.0282, *wR2* = 0.0658; [I > 2σ(I)]). In addition, the Si atom goes non positive definite and in the final difference density map, an extremely high peak of 26.74 e/Å^3 appears at 0.03 Å from Si.

As a blind test, we also refined the data obtained on $\mathbf{2}^{\mathbf{Si}}$ by Schweizer *et al.* [S8] as **2**. If the central Si atom (Si2) is refined as a Ge atom, the figures of merit become significantly worse: *R1* = 0.1638, *wR2* = 0.3660 (instead of *R1* = 0.0311, *wR2* = 0.0510; [I > 2σ(I)]).

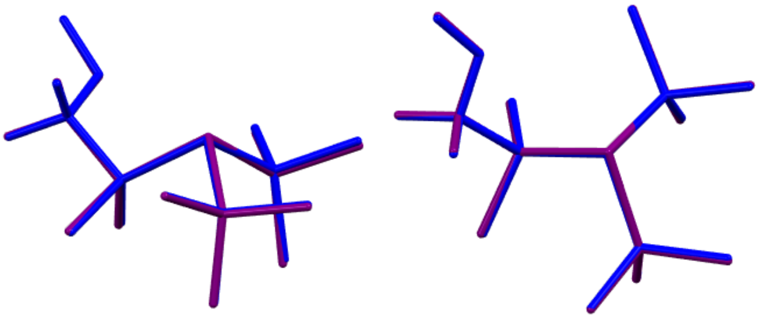

Figure S28: Overlay of the crystal structures of **2** (purple) and $\mathbf{2}^{\mathbf{Si}}$ (blue), shown in two different orientations.

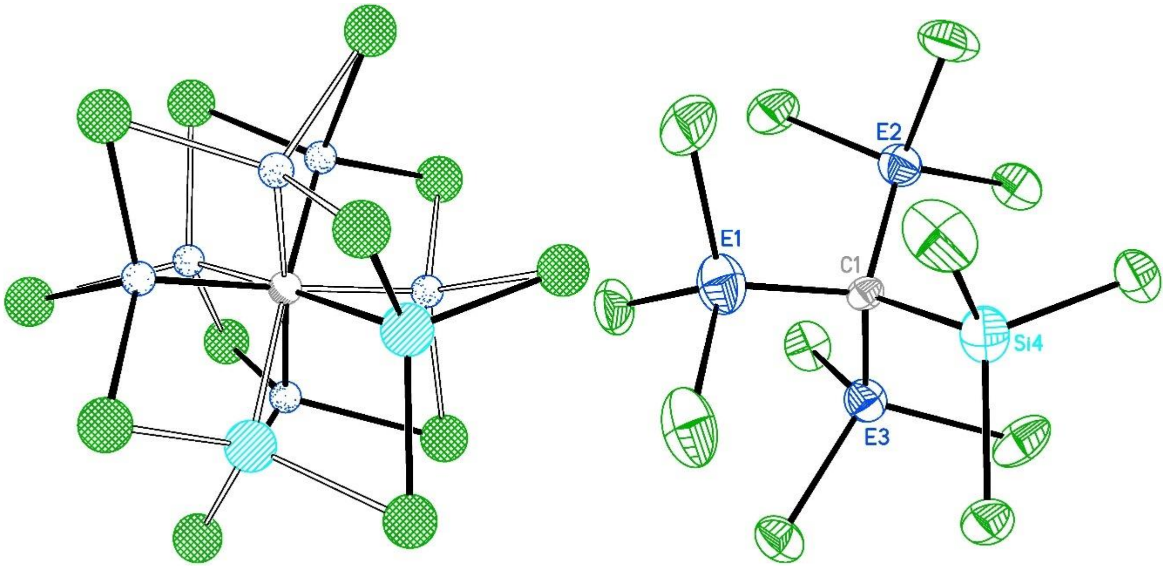

Figure S29: Molecular structure of [nBu$_4$N][(Cl$_3$Si)$_3$CAlCl$_3$], in the solid state. Displacement ellipsoids are shown at the 50% probability level. The [nBu$_4$N]$^+$ cation is omitted for clarity. Symmetry operator for generating equivalent atoms: x, –y+3/2, z. Color code: green = Cl, light blue = Si, dark blue = Al or Si. **CCDC: 2105158.**

The cation [nBu$_4$N]$^+$ and anion [(Cl$_3$Si)$_3$CAlCl$_3$]$^-$ are located on a mirror plane. Left: In the anion, the Si and Al atoms are disordered over two equally occupied positions, the overlay of both generating a cube. The mutually disordered Si and Al atoms were constrained to have the same coordinates and displacement parameters. The site occupation factors were refined so that the sum for the Al atoms in one anion is 1 and the sum of the Si atoms is 3. Right: The Al atom in each tetrahedral unit is disordered over three positions through rotation about the C(1)–Si(4) axis. Site occupation factors: E(1) = 0.182(4) Al, E(2) = 0.179(4) Al, and E(3) = 0.139(4) Al.

Si and Al are not distinguishable using the applied method since their electron count differs by only 1 e$^-$. Nevertheless, the presence of the cation [nBu$_4$N]$^+$ (not shown) proves that also an anionic species must be present. This rules out that all four –ECl$_3$ moieties contain fully occupied Si atoms. Since [(Cl$_3$Si)$_3$C]$^-$ adopts a trigonal-planar geometry in the solid state, the observed tetragonally coordinated C atom rules out the possibility that the investigated crystal consists of unreacted, disordered [(Cl$_3$Si)$_3$C]$^-$.[S2,S11] Furthermore, the presence of a four-coordinate Al atom is evidenced by ^{27}Al NMR spectroscopy.

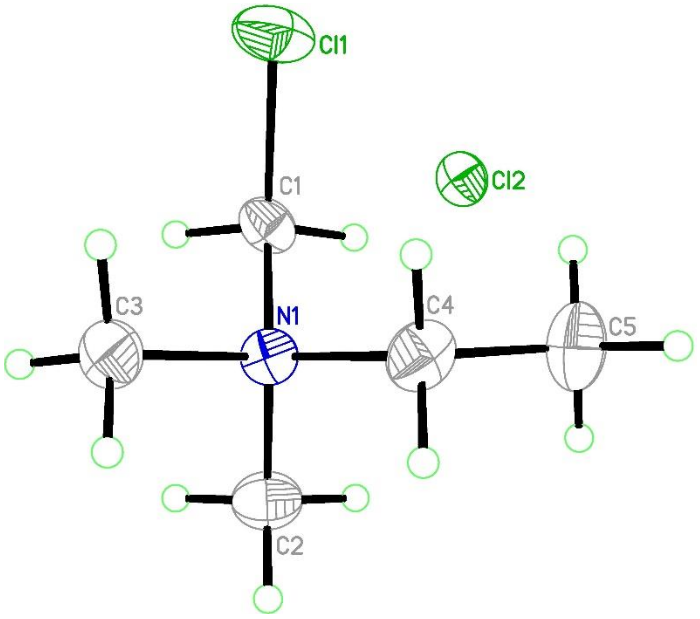

Figure S30: Molecular structure of [Me$_2$EtNCH$_2$Cl]Cl, in the solid state. Displacement ellipsoids are shown at the 50% probability level. **CCDC: 2105159.**

The absolute structure could be determined: Flack-x-parameter 0.13(10).

Table S1: Selected crystallographic data for **2**, [*n*Bu$_4$N][(Cl$_3$Si)$_3$CAlCl$_3$], and [Me$_2$EtNCH$_2$Cl]Cl.

	2	[*n*Bu$_4$N] [(Cl$_3$Si)$_3$CAlCl$_3$]	[Me$_2$EtNCH$_2$Cl]Cl
formula	$C_4H_{11}Cl_8GeNSi_3$	$C_{17}H_{36}AlCl_{12}NSi_3$	$C_5H_{13}Cl_2N$
M_r	513.60	395.56	158.06
T [K]	173(2)	173(2)	173(2)
radiation, λ [Å]	0.71073	0.71073	0.71073
crystal system	monoclinic	monoclinic	trigonal
space group	$P\,2_1/c$	$P\,2_1/m$	$R\,3c$
a [Å]	14.2948(6)	10.7853(14)	18.134(2)
b [Å]	10.5166(3)	11.6435(17)	18.134(2)
c [Å]	12.7899(5)	14.0828(18)	13.1827(13)
α [°]	90	90	90
β [°]	104.601(3)	91.747(11)	90
γ [°]	90	90	120
V [Å^3]	1860.64(12)	1767.7(4)	3754.2(9)
Z	4	2	18
D_{calcd} [g cm^{-3}]	1.833	1.486	1.258
F(000)	1008	808	1512
μ [mm^{-1}]	2.968	1.079	0.691
crystal size [mm]	0.190 x 0.160 x 0.160	0.150 x 0.050 x 0.050	0.500 x 0.300 x 0.250
rflns collected	35547	17906	2906
independent rflns (R_{int})	3495 (0.0440)	3499, (0.1562)	1549 (0.0343)
data/restraints/parameters	3495 / 0 / 154	3499 / 1 / 197	1549 / 1 / 73
GOF on F^2	1.221	1.101	0.995
R_1, wR_2 [I> 2σ(I)]	0.0282, 0.0658	0.1015, 0.2062	0.0284, 0.0664
R_1, wR_2 (all data)	0.0303, 0.0667	0.1764, 0.2402	0.0308, 0.0671
largest diff peak and hole [e Å^{-3}]	0.323, –0.372	1.677, –0.490	0.165, –0.162

4 EDX measurements

EDX measurements were carried out using an Amray 1830 Scanning Electron Microscope, controlled by an IXRF 550i controller, and the software *Iridium Ultra*.

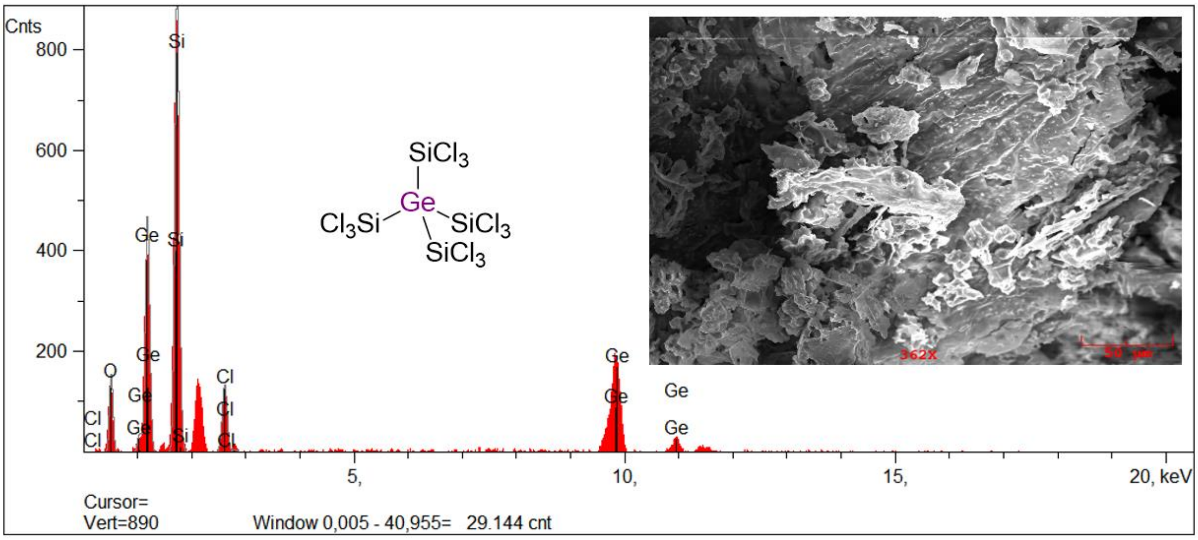

Figure S31: EDX spectrum of **1**.

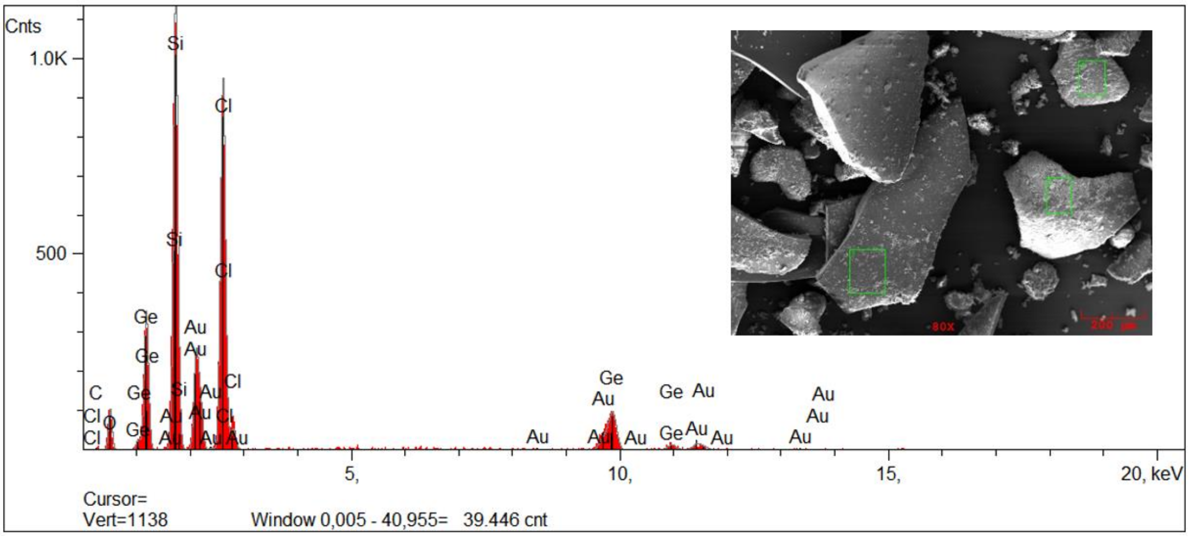

Figure S32: EDX spectrum obtained from a sample of single crystals of **2** after they were re-dissolved in CD_2Cl_2, stored at room temperature, and quenched with MeOH.

5 References

S1 F. Meyer-Wegner, A. Nadj, M. Bolte, N. Auner, M. Wagner, M. C. Holthausen and H.-W. Lerner, *Chem. - Eur. J.*, 2011, **17**, 4715–4719.

S2 I. Georg, J. Teichmann, M. Bursch, J. Tillmann, B. Endeward, M. Bolte, H.-W. Lerner, S. Grimme and M. Wagner, *J. Am. Chem. Soc.*, 2018, **140**, 9696–9708.

S3 J. Teichmann, C. Kunkel, I. Georg, M. Moxter, T. Santowski, M. Bolte, H.-W. Lerner, S. Bade and M. Wagner, *Chem. - Eur. J.*, 2019, **25**, 2740–2744.

S4 F. Stockhausen and L. Gattermann, *Ber. Dtsch. Chem. Ges.*, 1892, **25**, 3521–3525.

S5 G. R. Fulmer, A. J. M. Miller, N. H. Sherden, H. E. Gottlieb, A. Nudelman, B. M. Stoltz, J. E. Bercaw and K. I. Goldberg, *Organometallics*, 2010, **29**, 2176–2179.

S6 J. Burt, W. Levason, M. E. Light and G. Reid, *Dalton Trans.*, 2014, **43**, 14600–14611.

S7 J. Tillmann, L. Meyer, J. I. Schweizer, M. Bolte, H.-W. Lerner, M. Wagner and M. C. Holthausen, *Chem. - Eur. J.*, 2014, **20**, 9234–9239.

S8 J. I. Schweizer, M. G. Scheibel, M. Diefenbach, F. Neumeyer, C. Würtele, N. Kulminskaya, R. Linser, N. Auner, S. Schneider and M. C. Holthausen, *Angew. Chem., Int. Ed.*, 2016, **55**, 1782–1786.

S9 X.-A. Stoe & Cie, *Diffractometer control program system,* Stoe & Cie, Darmstadt, Germany, 2002.

S10 G. M. Sheldrick, *Acta Crystallogr., Sect. A: Found. Crystallogr.*, 2008, **64**, 112–122.

S11 U. Böhme, M. Gerwig, F. Gründler, E. Brendler and E. Kroke, *Eur. J. Inorg. Chem.*, 2016, 5028–5035.